

# Microwave Dielectric Properties of $(\text{Li}_{0.5}\text{Ln}_{0.5})\text{MoO}_4$ (Ln = Nd, Er, Gd, Y, Yb, Sm, and Ce) Ceramics

Li-Xia Pang,<sup>‡</sup> Di Zhou,<sup>§,†</sup> Jing Guo,<sup>§</sup> Zhen-Xing Yue,<sup>¶</sup> and Xi Yao<sup>§</sup>

<sup>‡</sup>Micro-optoelectronic Systems Laboratories, Xi'an Technological University, Xi'an, Shaanxi 710032, China

<sup>§</sup>Electronic Materials Research Laboratory, Key Laboratory of the Ministry of Education and International Center for Dielectric Research, Xi'an Jiaotong University, Xi'an, Shaanxi 710049, China

<sup>¶</sup>State Key Laboratory of New Ceramics and Fine Processing, Department of Materials Science and Engineering, Tsinghua University, Beijing 100084, China

In the present work, a series of scheelite-related  $(\text{Li}_{0.5}\text{Ln}_{0.5})\text{MoO}_4$  (Ln = Nd, Er, Gd, Y, Yb, Sm, and Ce) ceramics were prepared by using the solid-state reaction method. Except for the  $(\text{Li}_{0.5}\text{Yb}_{0.5})\text{MoO}_4$ , the other compositions were found to have a scheelite structure. Among all the compositions, the  $(\text{Li}_{0.5}\text{Sm}_{0.5})\text{MoO}_4$ ,  $(\text{Li}_{0.5}\text{Nd}_{0.5})\text{MoO}_4$ , and  $(\text{Li}_{0.5}\text{Ce}_{0.5})\text{MoO}_4$  ceramics were found to possess low sintering temperatures below melting point of aluminum (660°C) and be chemically compatible with Al. The relation between microwave dielectric properties and structure was analyzed by using the Shannon additive rule and bond-valence theory. This series of microwave dielectric ceramics might be candidate for low temperature co-fired ceramics technology.

## I. Introduction

WITH development of wireless and satellite communication, the low-temperature co-fired ceramics (LTCC) technology has played an important role due to its advantage in fabricating three-dimensional ceramic modules.<sup>1,2</sup> The LTCC technology requires microwave dielectric ceramic to be co-fired with metal electrode. In other words, the microwave dielectric ceramics used in the LTCC technology are required to have lower sintering temperatures than the melting points of inner electrodes and chemical compatibility.<sup>3,4</sup> Addition of sintering frits is the traditional method to lower the sintering temperatures of microwave dielectric ceramics.<sup>2–4</sup>

Recently, microwave dielectric ceramics with intrinsic low sintering temperatures have become more and more popular, especially in the  $\text{TeO}_2$ - and  $\text{MoO}_3$ -rich systems.<sup>5–7</sup> A number of  $\text{MoO}_3$ -rich oxide have been explored in the LTCC technology, such as the lyonsite  $(\text{Li}_2(\text{M}^{2+})_2\text{Mo}_3\text{O}_{12})$ ,  $\text{Li}_3(\text{M}^{3+})\text{Mo}_3\text{O}_{12}$ <sup>8</sup> and scheelite  $(\text{A}^{2+}\text{B}^{6+}\text{O}_4)$ ,  $(\text{A}_1+\text{A}_2^{3+})_{0.5}\text{B}^{6+}\text{O}_4$ , and  $(\text{A}_1+\text{A}_2^{3+})(\text{B}_1^{5+}\text{B}_2^{6+})\text{O}_4$  structured<sup>9–11</sup> systems. In fact, the scheelite structure with a general formula  $\text{ABO}_4$  is a ubiquitous adaptive structure type, like the perovskite structure in  $\text{ABO}_3$  system. In our previous work, a series of scheelite-structured microwave dielectric ceramics with ultra-low sintering temperatures have been explored, such as  $(\text{ABi})_{1/2}\text{MoO}_4$  (A = Li, Na, K, Rb, Ag),<sup>10</sup>  $(\text{A,Bi})(\text{Mo,V})\text{O}_4$  (A = Li, Na, K)<sup>11–13</sup>, and  $\text{Bi}(\text{Fe,V,Mo})\text{O}_4$ <sup>14</sup> systems. Some of them can be well densified at low sintering temperatures below melting point of aluminum (660°C) and are chemically com-

patible with Al. These results offers the opportunity to employ Al to replace Ag in the multi-layers co-fired devices and brings the LTCC technology to a novel field, so-called ultra-low temperature co-fired ceramics (ULTCC) technology. As shown in insert of Fig. 1, scheelite structure is quite adaptive and scheelite molybdate might possess low sintering temperature. In the scheelite crystal structure,  $\text{Mo}^{6+}$  cation is tetrahedrally coordinated to oxygen; thus, the structure may be regarded as made up of  $\text{A}^{2+}$  cations and  $\text{MoO}_4^{2-}$  anions. The A cation is coordinated to eight oxygens from eight different tetrahedra. Symmetry of the scheelite structure is body-centered tetragonal, but the structure may be regarded as pseudocubic.<sup>15,16</sup> All the A cations are equivalent, as are all  $\text{Mo}^{6+}$  cations and all oxygens. In the present work, the sintering behavior, microwave dielectric properties and its relation with the structure of the  $(\text{Li}_{0.5}\text{Ln}_{0.5})\text{MoO}_4$  (Ln = Nd, Er, Gd, Y, Yb, Sm, Ce) ceramics were studied in detail.

## II. Experimental Procedures

Reagent-grade starting materials were measured according to the stoichiometric compositions,  $(\text{Li}_{0.5}\text{Ln}_{0.5})\text{MoO}_4$  (Ln = Nd, Er, Gd, Y, Yb, Sm, Ce) (the RE-oxides were calcined at 800°C for 4 h in the muffle furnace before weighting). Powders were mixed and ball-milled (not the planetary milling) with stabilized zirconia media (Tosoh Ceramics, Tokyo, Japan) for 24 h. The powder mixtures were then calcined at 500°C–600°C for 4 h. The calcined powders were then vibratory milled with yttrium-stabilized zirconia media in nylon bottles for 24 h to increase the reactivity and homogeneity and following this the particulates were granulated with 2–5 wt. % acryloid polymer binder (Acrylic Resin, Rohm and Haas Chemicals LLC, Philadelphia, PA), and sieved through a mesh screen with 180  $\mu\text{m}$  openings. This was done to aid pressing and producing high green density. Then the powders were pressed into cylinders (12 mm in diameter and 6 mm in height) in a steel die under a uniaxial pressure of 100 MPa. After debinding (from room temperature to 500°C at a rate of 1°C/min and the incubation time is about 3 h) the samples were then sintered at various temperatures ranging from 510°C to 700°C for 2 h in ambient atmosphere. To investigate the chemical compatibility of these compounds with electrode metal powders, 20 wt. % Al powders were mixed with the different compounds and held at the sintering temperatures for 4 h.

The phase determination was made from X-ray diffraction (XRD) patterns obtained on a Scintag PADV and X2 diffractometers (Scintag Inc., Cupertino, CA) with  $\text{Cu K}_\alpha$  radiation ( $\lambda = 1.54 \text{ \AA}$ ). Prior to examination sintered pellets were crushed in a mortar to powder. Microstructures were

N. Alford—contributing editor

observed on the as-fired surfaces with a scanning electron microscopy (SEM) (Hitachi S-3000H, Hitachi High-Technologies Co., Tokyo, Japan). The apparent densities of ceramics were measured by Archimedes method.

Microwave dielectric properties were measured by the post-resonator method as suggested by Hakki and Coleman with a network analyzer (HP8510 Network Analyzer, Agilent, Hewlett-Packard, Palo Alto, CA). Temperature coefficient of resonant frequency (TCF) was determined using a zero thermal expansion cavity with programmable temperature chamber (Delta 9023, Delta Design, Poway, CA) in the temperature range of 25°C–85°C. The TCF was calculated by the following formula:

$$\tau_f = \frac{f_{85} - f_{25}}{f_{25} \times (85 - 25)} \times 10^6 \quad (1)$$

where  $f_{85}$  and  $f_{25}$  were the resonant frequencies at 85°C and 25°C, respectively.

### III. Results and Discussions

XRD patterns of scheelite-related  $(\text{Li}_{0.5}\text{Ln}_{0.5})\text{MoO}_4$  (Ln = Nd, Er, Gd, Y, Yb, Sm, and Ce) ceramic samples at various sintering temperatures and co-fired samples with 20 wt. % Al powders for  $(\text{Li}_{0.5}\text{Ce}_{0.5})\text{MoO}_4$  and  $(\text{Li}_{0.5}\text{Sm}_{0.5})\text{MoO}_4$  samples at 610°C are shown in Fig. 1. Besides the  $(\text{Li}_{0.5}\text{Yb}_{0.5})\text{MoO}_4$  samples, the other samples crystallized in a tetragonal scheelite structure. It was found that the  $(\text{Li}_{0.5}\text{Yb}_{0.5})\text{MoO}_4$  did not crystallize in a pure tetragonal scheelite structure, which can be formed in Saveleva *et al.*'s experiment using  $\text{Li}_2\text{MoO}_4$  and  $\text{Yb}_2(\text{MoO}_4)_3$  as the initial materials,<sup>17–20</sup> and this resulted in the overlapping and wideness of XRD peaks. From XRD patterns of the co-fired ceramics,  $(\text{Li}_{0.5}\text{Ce}_{0.5})\text{MoO}_4$  and  $(\text{Li}_{0.5}\text{Sm}_{0.5})\text{MoO}_4$  with 20 wt. % Al powders, it is observed that only the peaks of matrix materials and Al phases were revealed, which indicates that these three compounds are chemically compatible with Al at 610°C and might be useful for LTCC technology.

Cell parameters of the  $(\text{Li}_{0.5}\text{Ln}_{0.5})\text{MoO}_4$  (Ln = Nd, Er, Gd, Y, Yb, Sm, and Ce) ceramics were calculated from XRD data and the results are shown in Fig. 2(b). It is seen that  $a$  ( $= b$ ),  $c$  and cell volume all increased with the A site ionic radius while the  $a/c$  ratio decreased slightly, which indicates that the increase of A site ionic radius increases the  $c$  value more effectively than the  $a$  value. Combined with our

previous work,<sup>11–13</sup> it can be found that cell volume of the scheelite structured  $\text{ABO}_4$  can be remarkably increased by increasing the equivalent A site ionic radius.

Apparent densities of the scheelite-related  $(\text{Li}_{0.5}\text{Ln}_{0.5})\text{MoO}_4$  (Ln = Nd, Er, Gd, Y, Yb, Sm, and Ce) ceramic samples as a function of sintering temperature and the relative densities are shown in Fig. 3. Compared with the literatures' results,<sup>17,18</sup> the relative errors (listed in Table I) were smaller than 1.5% and it is acceptable. Almost all the relative densities are above 95% except  $(\text{Li}_{0.5}\text{Nd}_{0.5})\text{MoO}_4$  and  $(\text{Li}_{0.5}\text{Yb}_{0.5})\text{MoO}_4$ , which is 90.0% and 83.1%, respectively. The small relative density of  $(\text{Li}_{0.5}\text{Yb}_{0.5})\text{MoO}_4$  ceramic might be attributed to mixed phases. Considering melting point of Al around 660°C, only the  $(\text{Li}_{0.5}\text{Ce}_{0.5})\text{MoO}_4$ , and  $(\text{Li}_{0.5}\text{Sm}_{0.5})\text{MoO}_4$  samples might be candidates for ULTCC technology using Al as inner electrode material. As shown in Fig. 3(b), densification temperatures of the  $(\text{Li}_{0.5}\text{Ln}_{0.5})\text{MoO}_4$  ceramics decreases with ionic radius of Ln. The combination of covalent and ionic bonds determines melting points of the complex oxides and indirectly affects their densification temperatures. It is understandable that the electrostatic force and the shared electrons become weak as the distances between atoms increase, which results in the decrease of melting and densification temperatures.

SEM images of the  $(\text{Li}_{0.5}\text{Sm}_{0.5})\text{MoO}_4$  ceramic sintered at 650°C/2 h,  $(\text{Li}_{0.5}\text{Ce}_{0.5})\text{MoO}_4$  ceramic sintered at 610°C/2 h,  $(\text{Li}_{0.5}\text{Er}_{0.5})\text{MoO}_4$  ceramic sintered at 810°C/2 h and  $(\text{Li}_{0.5}\text{Yb}_{0.5})\text{MoO}_4$  ceramic sintered at 830°C/2 h are shown in Fig. 4. Dense and homogeneous microstructures are observed for the  $(\text{Li}_{0.5}\text{Sm}_{0.5})\text{MoO}_4$ ,  $(\text{Li}_{0.5}\text{Ce}_{0.5})\text{MoO}_4$ , and  $(\text{Li}_{0.5}\text{Er}_{0.5})\text{MoO}_4$  ceramics. However, for  $(\text{Li}_{0.5}\text{Yb}_{0.5})\text{MoO}_4$  ceramic, the microstructure looks porous and it might be caused by the amorphous matters.

Microwave dielectric permittivities and  $Q \times f$  values as a function of sintering temperature are shown in Fig. 5. It is seen that as sintering temperature increases, microwave dielectric permittivity increases first and then reaches a saturated value as there is an elimination of the pores. The influence of the porosity on the microwave permittivity could be eliminated by applying Bosman and Havinga's correction<sup>21,22</sup> as shown in Eq. (2)

$$\varepsilon_{\text{Bosman}} = \varepsilon_m (1 + 1.5P) \quad (2)$$

where  $\varepsilon_{\text{Bosman}}$  and  $\varepsilon_m$  are corrected and measured values of permittivity, respectively.  $P$  is the fractional porosity. The porosity

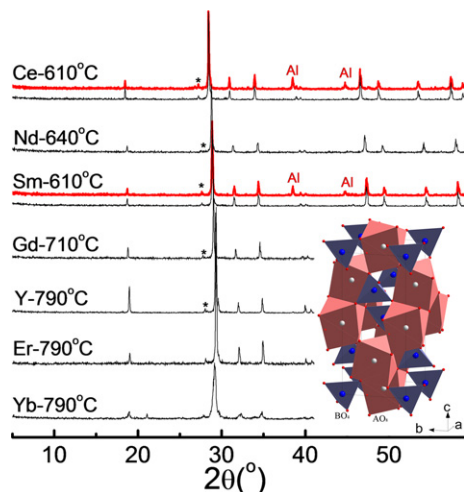


**Fig. 1.** XRD patterns of the scheelite-related  $(\text{Li}_{0.5}\text{Ln}_{0.5})\text{MoO}_4$  (Ln = Nd, Er, Gd, Y, Yb, Sm, Ce) ceramic samples at various sintering temperatures and co-fired samples with 20 wt.% Al powders for  $(\text{Li}_{0.5}\text{Ce}_{0.5})\text{MoO}_4$  and  $(\text{Li}_{0.5}\text{Sm}_{0.5})\text{MoO}_4$  samples at 610°C (\*—extraneous instrumental peak).

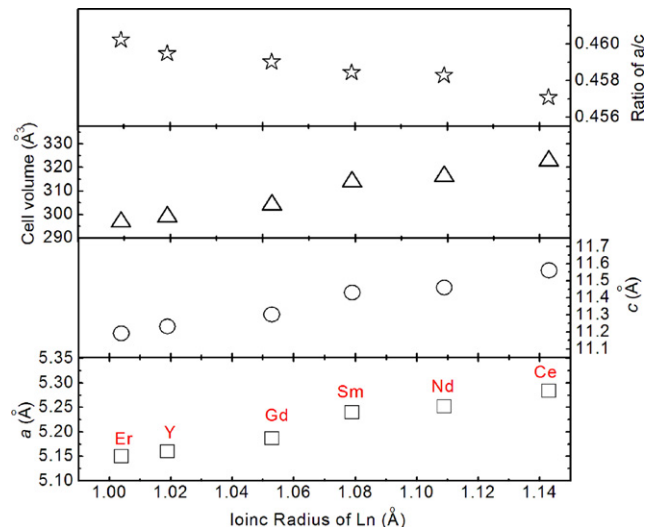


**Fig. 2.** Schematic illustrations of scheelite crystal structure  $(\text{ABO}_4)$  (a), and cell parameters of the  $(\text{Li}_{0.5}\text{Ln}_{0.5})\text{MoO}_4$  (Ln = Nd, Er, Gd, Y, Sm, Ce) ceramics as a function of the ionic radius of Ln elements.

**Table I. Sintering Temperatures and Microwave Dielectric Properties of the  $(\text{Li}_{0.5}\text{Ln}_{0.5})\text{MoO}_4$  Ceramics**

Composition	R(Ln)	S.T. (°C)	$\epsilon_r$	$\epsilon_{\text{core}}$	$Q \times f$ (GHz)	TCF (ppm/°C)	Reference
$(\text{Li}_{0.5}\text{Yb}_{0.5})\text{MoO}_4$	0.9525	820	16.3	20.4	6350	+53	This work
$(\text{Li}_{0.5}\text{Er}_{0.5})\text{MoO}_4$	0.962	800	18.6	19.1	10 650	+186	This work
$(\text{Li}_{0.5}\text{Y}_{0.5})\text{MoO}_4$	0.9695	780	18.8	19.1	10 400	+193	This work
$(\text{Li}_{0.5}\text{Gd}_{0.5})\text{MoO}_4$	0.9865	750	19.5	20.0	3940	+209	This work
$(\text{Li}_{0.5}\text{Sm}_{0.5})\text{MoO}_4$	0.9995	640	19.9	20.5	4570	+231	This work
$(\text{Li}_{0.5}\text{Nd}_{0.5})\text{MoO}_4$	1.0145	660	20.3	23.7	3000	+235	This work
$(\text{Li}_{0.5}\text{Ce}_{0.5})\text{MoO}_4$	1.0315	580	20.6	21.5	1990	+228	This work
$(\text{Li}_{0.5}\text{Bi}_{0.5})\text{MoO}_4$	1.045	560	41.7		3200	+240	10
$(\text{Na}_{0.5}\text{Bi}_{0.5})\text{MoO}_4$	1.175	590	34.4		12 300	+43	10
$(\text{Ag}_{0.5}\text{Bi}_{0.5})\text{MoO}_4$	1.225	690	30.4		12 600	+57	10

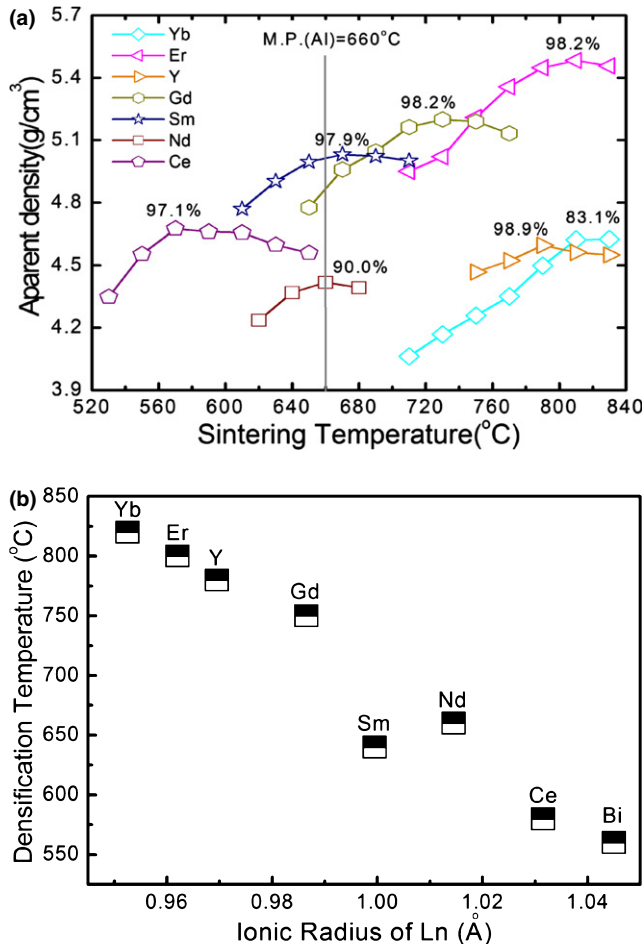


**Fig. 3.** Apparent densities of the scheelite-related  $(\text{Li}_{0.5}\text{Ln}_{0.5})\text{MoO}_4$  (Ln = Nd, Er, Gd, Y, Yb, Sm, Ce) ceramic samples as a function of sintering temperature (a) and densification temperatures as a function of ionic radius of Ln ions (b).

corrected permittivities are shown in Table I. At the microwave region, polarizability is the sum of both ionic and electronic components.<sup>23</sup> Shannon<sup>24</sup> suggested that molecular polarizabilities of complex substances can be estimated by summing the polarizabilities of the constituent ions. Then the polarizabilities  $\alpha_x$  of  $(\text{Li}_{0.5}\text{Ln}_{0.5})\text{MoO}_4$  could be obtained as follows:

$$\alpha_x = 0.5 \times \alpha_{\text{Li}^+} + 0.5 \times \alpha_{\text{Ln}^{3+}} + \alpha_{\text{Mo}^{6+}} + 4 \times \alpha_{\text{O}^{2-}} \quad (3)$$

where  $\alpha_{\text{Li}^+}$ ,  $\alpha_{\text{Ln}^{3+}}$ ,  $\alpha_{\text{Mo}^{6+}}$  and  $\alpha_{\text{O}^{2-}}$  are the respective polarizabilities of  $\text{Li}^+$ ,  $\text{Ln}^{3+}$ ,  $\text{Mo}^{6+}$ , and  $\text{O}^{2+}$  ions.

Using the Clausius–Mosotti relation, the molecular dielectric polarizability  $\alpha_x$  and the molar volume  $V_x$ , dielectric con-

stant can be calculated as following:

$$\epsilon_x = \frac{3V_x + 8\pi\alpha_x}{3V_x - 4\pi\alpha_x} \quad (4)$$

where  $V_x$  is the cell volume and  $\epsilon_x$  is the calculated dielectric permittivity. All the results are listed in Table I. As seen from Fig. 6(a), microwave dielectric permittivity increased almost linearly with the Ln ionic radius, which resulted from the increasing Ln ionic polarization. Meanwhile,  $Q \times f$  value decreased with the Ln ionic radius, which could be attributed to the increasing intrinsic dielectric loss caused by the stronger oscillations.<sup>25</sup> Temperature coefficients of resonant frequency (TCF) could be defined as following:

$$\text{TCF} = -\alpha_1 - \frac{1}{2} \tau_\epsilon \quad (5)$$

where  $\alpha_1$  is the linear thermal expansion coefficient and  $\tau_\epsilon$  is the temperature coefficient of permittivity. Since  $\alpha_1$  of oxide ceramic is known to be in the range of +10 ppm/°C and assuming that  $\alpha_1$  of the  $(\text{Li}_{0.5}\text{Ln}_{0.5})\text{MoO}_4$  ceramic is independent on  $x$  value, TCF mainly depends on  $\tau_\epsilon$ . Using the Clausius–Mosotti equation, Bosman and Havinga<sup>21</sup> derived an expression for  $\tau_\epsilon$  at a constant pressure, as follows:

$$\begin{aligned} \tau_\epsilon &= \frac{1}{\epsilon} \left( \frac{\partial \epsilon}{\partial T} \right)_P = \frac{(\epsilon - 1)(\epsilon + 2)}{\epsilon} (A + B + C) \\ &= \left( \epsilon - \frac{2}{\epsilon} + 1 \right) (A + B + C) \end{aligned} \quad (6)$$

$$\begin{aligned} A &= \frac{1}{3V} \left( \frac{\partial V}{\partial T} \right)_P, B = \frac{1}{3\alpha_m} \left( \frac{\partial \alpha_m}{\partial V} \right)_T \left( \frac{\partial V}{\partial T} \right)_P, \\ C &= \frac{1}{3\alpha_m} \left( \frac{\partial \alpha_m}{\partial T} \right)_V \end{aligned}$$

The sum of the  $A$  and  $B$  terms is approximately  $6 \pm 1$  ppm/°C. For term  $C$ , the suggested value is in the range of  $-1$  to  $-10$  ppm/°C. The term  $C$  represents the direct dependence of the polarizability on temperature. Although TCF values of all the microwave dielectric ceramics collected by Sebastian *et al.*<sup>1</sup> seemed to scatter randomly, some simple rules can be obtained in solid solutions and oxides with the same crystal structure. For the  $(\text{Li}_{0.5}\text{Ln}_{0.5})\text{MoO}_4$  ceramics here with scheelite structure,  $A$ ,  $B$ , and  $C$  had very similar values and absolute value of TCF values mainly depended on  $\epsilon_r$ . As seen from Fig. 6(b), TCF values of the  $(\text{Li}_{0.5}\text{Ln}_{0.5})\text{MoO}_4$  ceramics increased almost linearly with Ln ionic radius first and then reached a saturated value around +230 ppm/°C. Bond valence considerations provided a useful way of examining bonding between every atom in particular structures and it was found to be useful to determine the TCF trend in  $\text{Bi}_2\text{O}_3$ - $\text{MoO}_3$  system. The bond valences are obtained via the relation:

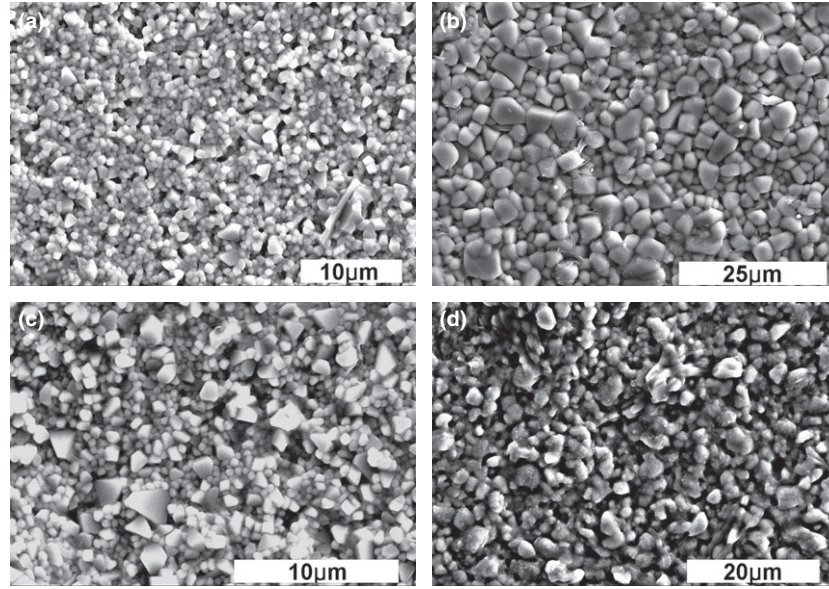


Fig. 4. SEM images of the  $(Li_{0.5}Sm_{0.5})MoO_4$  ceramic sintered at  $650^\circ C/2$  h (a),  $(Li_{0.5}Ce_{0.5})MoO_4$  ceramic sintered at  $610^\circ C/2$  h (b),  $(Li_{0.5}Er_{0.5})MoO_4$  ceramic sintered at  $810^\circ C/2$  h (c) and  $(Li_{0.5}Yb_{0.5})MoO_4$  ceramic sintered at  $830^\circ C/2$  h (d).

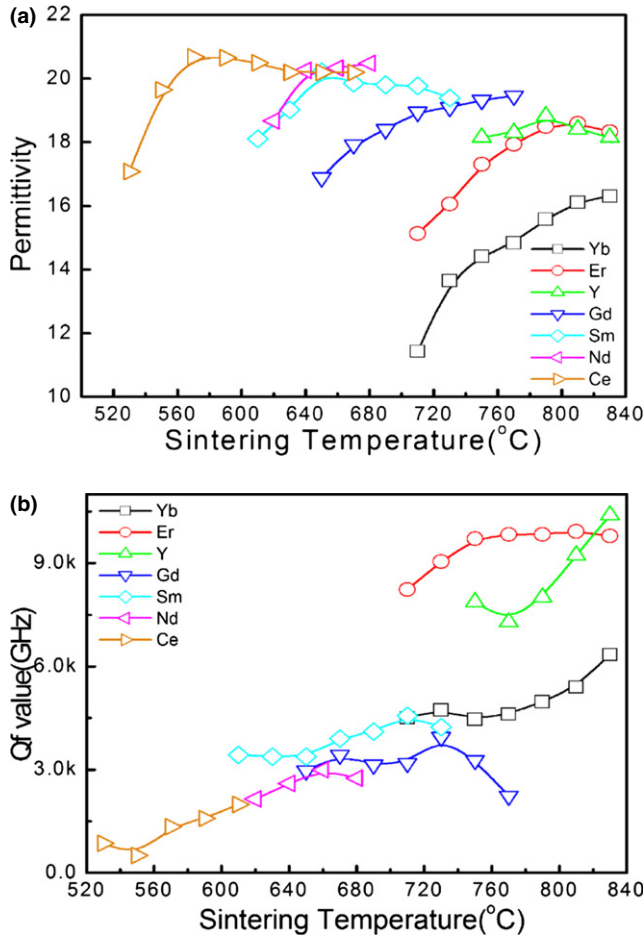


Fig. 5. Microwave dielectric permittivities (a) and  $Q \times f$  values (b) of the scheelite-related  $(Li_{0.5}Ln_{0.5})MoO_4$  ( $Ln = Nd, Er, Gd, Y, Yb, Sm, Ce$ ) ceramic samples as a function of sintering temperature.

$$v_{ij} = \exp\left(\frac{R_0 - d_{ij}}{0.37}\right) \quad (7)$$

where the  $R_0$  is a valence bond parameter and  $d_{ij}$  is the actual distance between two atoms.<sup>26</sup> The bond-valence

parameters were taken from tabulated  $R_0$  values given by Brown, Altermatt,<sup>27</sup> Brese and O'Keeffe.<sup>28</sup> In our case, the data are listed in Table II. Valences bond sums are obtained by simply summing over all neighbors at each site:

$$V_{ij} = \sum_j v_{ij} \quad (8)$$

Results presented here are based on the refined atomic coordinates obtained from literatures.<sup>17–20,29</sup> Results for metal site valence sums are presented in Fig. 6(c) and variations from the expected formal valence of about 5%–10% are common in bond-valence calculations. It is seen that the calculated valences of Mo, O, and Li decreased linearly with the Ln ionic radius while the valences of Ln ions decreased. Valence deviation suggests the compressing or expanding of ions, which also represents the unstable status of a cation. It is believed that the valence deviations of ions with large polarizations dominate the TCF values. Here, a so-called weighting function of bond-valence deviation for  $(Li_{0.5}Ln_{0.5})MoO_4$  systems is defined as following:

$$0.5 \times (|V_{Li} - 1| \times \rho_{Li} + |V_{Ln} - 3| \times \rho_{Ln}) + |V_{Mo} - 6| \times \rho_{Mo} + 4 \times |V_{O} - 3| \times \rho_O \quad (9)$$

Microwave dielectric permittivity and TCF value of  $(Li_{0.5}Ln_{0.5})MoO_4$  ceramic as a function of weighting function of bond-valence deviation are shown in Fig. 6(d). It is found that both the permittivity and TCF value are almost linearly to the weighting function. Generally, TCF values of the  $(Li_{0.5}Ln_{0.5})MoO_4$  ceramics are all large positive and not suitable for temperature stable devices.

#### IV. Conclusions

In the present work, a series of  $(Li_{0.5}Ln_{0.5})MoO_4$  ( $Ln = Nd, Er, Gd, Y, Yb, Sm, Ce$ ) ceramics were prepared by using the solid-state reaction method. All the ceramic samples could be well densified below  $820^\circ C$ . Especially, the  $(Li_{0.5}Sm_{0.5})MoO_4$ ,  $(Li_{0.5}Nd_{0.5})MoO_4$ , and  $(Li_{0.5}Ce_{0.5})MoO_4$  ceramics have sintering temperatures below the melting point of aluminum ( $660^\circ C$ ) and are chemically compatible with Al. Besides the  $(Li_{0.5}Yb_{0.5})MoO_4$  ceramics, the other samples

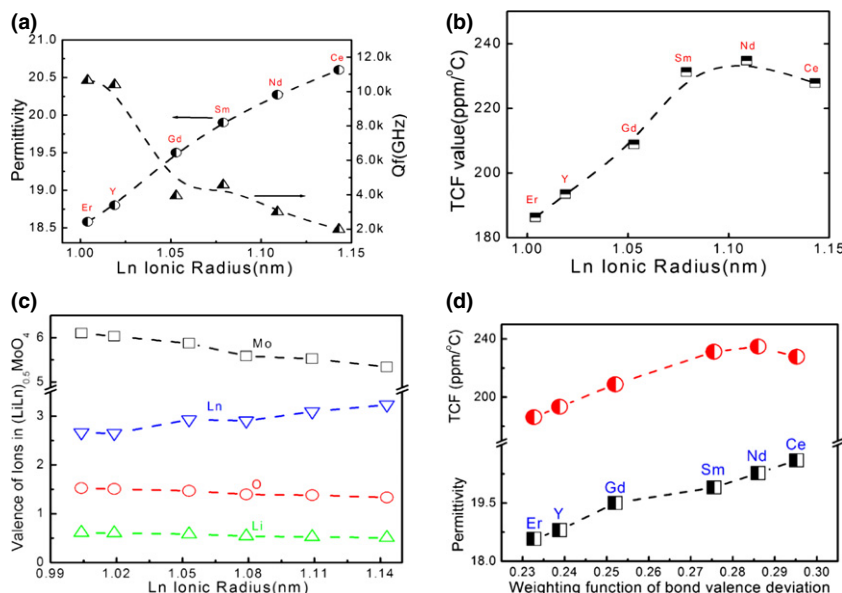


**Fig. 6.** Microwave dielectric permittivity and  $Q \times f$  value (a), TCF (b) and calculated ionic valence (c) as a function of radius of Ln, and permittivity and TCF as a function of the bond-valence deviation (d).

**Table II.** Bond-Valence Parameters Taken From Literatures Ref. [27] and [28]

Bond type	$Li^{+}-O$	$Bi^{3+}-O$	$Yb^{3+}-O$	$Y^{3+}-O$	$Er^{3+}-O$
$R_0$ (nm)	0.1466	0.2094	0.1966	0.2020	0.1989
$Nd^{3+}-O$	$Gd^{3+}-O$	$Sm^{3+}-O$	$Ce^{3+}-O$	$Mo^{6+}-O$	O-O
0.2106	0.2065	0.2088	0.2151	0.1907	0.148

were found to crystallize in a pure scheelite structure. Microwave dielectric permittivity of the scheelite phase was found to increase linearly with Ln ionic radius while the  $Q \times f$  value decreased. Temperature coefficient of resonant frequency was found to depend on the equivalent bond-valence deviation of ions in  $(Li_{0.5}Ln_{0.5})MoO_4$ . This series of low-temperature firing ceramics might be useful in the LTCC technology.

### Acknowledgments

This work was supported by National Science Foundation of China (51202182, 51202178), the Fundamental Research Funds for the Central University, the International Cooperation Project of Shaanxi Province (2013KW12-04), the State Key Laboratory of New Ceramic and Fine Processing Tsinghua University, and the 111 Project of China (B14040). The SEM work was partially done at International Center for Dielectric Research (ICDR), Xi'an Jiaotong University, Xi'an, China and the authors thank Ms. Yan-Zhu Dai for her help in using SEM.

### References

- M. T. Sebastian and H. Jantunen, "Low Loss Dielectric Materials for LTCC Applications: A Review," *Int. Mater. Rev.*, **53**, 57–90 (2008).
- M. Valant and D. Suvorov, "Chemical Compatibility Between Silver Electrodes and low-Firing Binary-Oxide Compounds: Conceptual Study," *J. Am. Ceram. Soc.*, **83**, 2721–9 (2000).
- R. J. Cava, "Dielectric Materials for Applications in Microwave Communications," *J. Mater. Chem.*, **11**, 54–62 (2001).
- D. Zhou, J. Guo, X. Yao, L. X. Pang, Z. M. Qi, and T. Shao, "Phase Evolution and Microwave Dielectric Properties of  $(Li_{0.5}Bi_{0.5})(WMo)O_4$  Ceramics With Ultralow Sintering Temperatures," *Funct. Mater. Lett.*, **5**, 1250042, 5pp (2012).
- D. K. Kwon, M. T. Lanagan, and T. R. Shrout, "Microwave Dielectric Properties and low-Temperature Cofiring of  $BaTe_2O_9$  With Aluminum Metal Electrode," *J. Am. Ceram. Soc.*, **88**, 3419–22 (2005).
- M. Udovic, M. Valant, and D. Suvorov, "Phase Formation and Dielectric Characterization of the  $Bi_2O_3$ - $TeO_2$  System Prepared in an Oxygen Atmosphere," *J. Am. Ceram. Soc.*, **87**, 591–7 (2004).
- D. Zhou, H. Wang, L. X. Pang, C. A. Randall, and X. Yao, " $Bi_2O_3$ - $MoO_3$  Binary System: An Alternative Ultra low Sintering Temperature Microwave Dielectric," *J. Am. Ceram. Soc.*, **92**, 2242–6 (2009).

<sup>8</sup>D. Zhou D, C. A. Randall, L. X. Pang, H. Wang, X. G. Wu, J. Guo, G. Q. Zhang, L. Shui, and X. Yao, "Microwave Dielectric Properties of  $Li_2(M^{2+})_2Mo_3O_{12}$  and  $Li_3(M^{3+})Mo_3O_{12}$  ( $M = Zn, Ca, Al, \text{ and } In$ ) Lyonsite-Related-Terminate Ceramics With Ultra-Low Sintering Temperatures," *J. Am. Ceram. Soc.*, **94**, 802–5 (2011).

<sup>9</sup>S. H. Yoon, D. W. Kim, S. Y. Cho, and K. S. Hong, "Investigation of the Relations Between Structure and Microwave Dielectric," *J. Eur. Ceram. Soc.*, **26**, 2051–4 (2006).

<sup>10</sup>D. Zhou, C. A. Randall, L. X. Pang, H. Wang, J. Guo, G. Q. Zhang, Y. Wu, K. T. Guo, L. Shui, and X. Yao, "Microwave Dielectric Properties of  $(ABi)_{1/2}MoO_4$  ( $A = Li, Na, K, Rb, Ag$ ) Type Ceramics With Ultra-low Firing Temperatures," *Mater. Chem. Phys.*, **129**, 688–92 (2011).

<sup>11</sup>D. Zhou, L. X. Pang, H. Wang, J. Guo, X. Yao, and C. A. Randall, "Phase Transition, Raman Spectra, Infrared Spectra, Band gap and Microwave Dielectric Properties of low Temperature firing  $(Na_{0.5x}Bi_{1-0.5x})(Mo_xV_{1-x})O_4$  Solid Solution Ceramics With Scheelite Structures," *J. Mater. Chem.*, **21**, 18412–20 (2011).

<sup>12</sup>D. Zhou, L. X. Pang, J. Guo, H. Wang, X. Yao, and C. A. Randall, "Phase Evolution, Phase Transition, Raman Spectra, Infrared Spectra, and Microwave Dielectric Properties of low Temperature Firing  $(K_{0.5x}Bi_{1-0.5x})(Mo_xV_{1-x})O_4$  Ceramics With Scheelite Related Structure," *Inorg. Chem.*, **50**, 12733–8 (2011).

<sup>13</sup>D. Zhou, L. X. Pang, W. G. Qu, C. A. Randall, J. Guo, Z. M. Qi, T. Shao, and X. Yao, "Dielectric Behavior, Band gap, in Situ X-ray Diffraction, Raman and Infrared Study on  $(1-x)BiVO_4$ - $X(Li_{0.5}Bi_{0.5})MoO_4$  Solid Solution," *RSC Adv.*, **3**, 5009–14 (2013).

<sup>14</sup>D. Zhou, L. X. Pang, J. Guo, Z. M. Qi, T. Shao, X. Yao, and C. A. Randall, "Phase Evolution, Phase Transition, and Microwave Dielectric Properties of Scheelite Structured  $xBi(Fe_{1/3}Mo_{2/3})O_4$ - $(1-x)BiVO_4$  ( $0.0 \leq x \leq 1.0$ ) low Temperature Firing Ceramics," *J. Mater. Chem.*, **22**, 21412–9 (2012).

<sup>15</sup>A. W. Sleight and W. J. Linn, "Olefin Oxidation Over Oxide Catalysts With the Scheelite Structure," *Ann. New York Academy Sci.*, **272**, 22–44 (1976).

<sup>16</sup>A. W. Sleight, "Accurate Cell Dimensions for  $ABO_4$  Molybdates and Tungstates," *Acta Crystallogr.*, **28**, 2899–902 (1972).

<sup>17</sup>P. V. Klevtsov and L. P. Kozeeva, "Synthesis of Double Lithium Molybdates of Rare Earths and Yttrium," *Inorg. Mater. (Engl. Transl.)*, **5**, 1571–2 (1969).

<sup>18</sup>M. V. Saveleva, I. V. Shakhno, and V. E. Plushchev, "Synthesis and Properties of Alkali and Rare Earth Molybdates," *Inorg. Mater.*, **6**, 1466–70 (1970).

<sup>19</sup>M. V. Mokhosoev, E. I. Getman, and F. P. Alekseev, "Double Molybdates of Alkali and Rare-Earth Elements  $MeLn(MoO_4)_2$ ," *Dokl. Akad. Nauk SSSR*, **185**, 361–2 (1969).

<sup>20</sup>V. Volkov, C. Cascales, A. Kling, and C. Zaldo, "Growth, Structure and Evaluation of Laser Properties of  $LiYb(MoO_4)$  Single Crystal," *Chem. Mater.*, **17**, 291–300 (2005).

<sup>21</sup>A. J. Bosman and E. E. Havinga, "Temperature Dependence of Dielectric Constants of Cubic Ionic Compounds," *Phys. Rev.*, **129**, 1593–600 (1963).

<sup>22</sup>D. W. Kim, I. T. Kim, B. Park, K. S. Hong, and J. H. Kim, "Microwave Dielectric Properties of  $(1-x)Cu_3Nb_2O_8$ - $xZn_3Nb_2O_8$  Ceramics," *J. Mater. Res.*, **16**, 1465–70 (2001).

<sup>23</sup>A. Heydweiller, "Dielektrizitätskonstante und Refraktion Fester Salze," *Z. Phys.*, **3**, 308–17 (1920).

<sup>24</sup>R. D. Shannon, "Dielectric Polarizabilities of Ions in Oxides and Fluorides," *J. Appl. Phys.*, **73**, 348–66 (1993).

<sup>25</sup>D. Zhou, H. Wang, Q. P. Wang, X. G. Wu, J. Guo, G. Q. Zhang, L. Shui, X. Yao, C. A. Randall, and H. C. Liu, "Microwave Dielectric Properties and Raman Spectroscopy of Scheelite Solid Solution  $[(Li_{0.5}Bi_{0.5})_{1-x}Ca_x]MoO_4$  Ceramics With Ultra-low Sintering Temperatures," *Funct. Mater. Lett.*, **3**, 253–7 (2010).

<sup>26</sup>M. O'Keefe and N. E. Brese, "Atom Sizes and Bond Lengths in Molecules and Crystals," *J. Am. Chem. Soc.*, **113**, 3226–9 (1991).

<sup>27</sup>I. D. Brown and D. Altermatt, "Bond-Valence Parameters Obtained From a Systematic Analysis of the Inorganic Crystal Structure Database," *Acta Cryst. B*, **41**, 244–7 (1985).

<sup>28</sup>N. E. Brese and M. O'Keefe, "Bond-Valence Parameters for Solids," *Acta Cryst.*, **47**, 192–7 (1991).

<sup>29</sup>A. A. Evdokimov, V. K. Trunov, and B. M. Sokolovskii, "Double Molybdates and Tungstates of Alkaline and Rare-Earth Elements, Synthesized at High-Pressure," *Zh. Neorg. Khim.*, **25**, 710–2 (1980). □